Journal of Constructional Steel Research

Volume 64, Issue 9, September 2008, Pages 997–1007

Imperial College Centenary

Earthquake testing and response analysis of concentrically-braced sub-frames

- B.M. Broderick[a], A.Y. Elghazouli[b], J. Goggins[c]
- [a] Department of Civil, Structural and Environmental Engineering, Museum Building, Trinity College Dublin, Ireland
- [b] Department of Civil and Environmental Engineering, Imperial College, London, SW7 2BU, UK
- [c] Buro Happold Ltd, London, UK

Abstract

The results of shake table tests on three concentrically-braced sub-frames are compared with a series of correlative inelastic analyses. Both transient time-history and nonlinear static (pushover) analyses are considered. The lateral resistance of the test frames is provided by a pair of cold-formed tubular steel members. The brace cross-section is varied between tests to investigate the influence of brace slenderness on the stiffness, resistance and ductility displayed by the frame under strong earthquake loading. Response simulations using a two-dimensional analytical model of the test frame are compared with the experimental results. Brace strengths and elastic test frame properties established in complementary static tensile tests and low-level shake table tests, respectively, are used to determine model input data. The transient acceleration and displacement response of the frames calculated in nonlinear time-history analyses are compared with corresponding experimental measurements. The base shear–frame drift relationship is calculated using pushover analyses that consider either the resistance of both frame braces or the tension brace alone. These are compared with the experimental hysteretic response of the test frame. On the whole, the analytical results are observed to agree well with the experimental results, especially with respect to brace tension forces and frame base shear. Cases where the experimental and analytical responses deviate are identified and the implications for earthquake response assessment and design are discussed.

Keywords

- Concentrically-braced frames;
- Shake table testing;
- Earthquake analysis;
- Time-history analysis;
- Pushover analysis

1. Introduction

When concentrically-braced frames are subjected to earthquake loading, the brace members are subjected to alternating tension and compression loads. The complex asymmetric response displayed under these conditions has prompted several investigations of the cyclic behaviour of bracing members (e.g.[1-9]). Most of these have been based on quasi-static cyclic tests conducted under pre-defined displacement histories for specific ranges of member slenderness, with comparatively fewer studies performed under realistic dynamic loading conditions.

In terms of design procedures, seismic codes of practice typically adopt the general philosophy of capacity design. In the case of concentrically-braced frames, capacity design normally implies the use of diagonal bracing members as the main dissipative elements, whilst providing adequate overstrength factors for other frame members and components to ensure compliance with the selected failure mode. Dissipative designs, such as Eurocode 8 [10] rely on the capability of parts of the structure (dissipative zones) to resist earthquake actions beyond their elastic range. In the case of concentrically-braced frames, Eurocode 8 assumes that only tension diagonals participate in the lateral resistance of earthquake-induced loading, and hence, in these structures dissipative zones are mainly located in the tension diagonals. This approach is different from that followed in other seismic codes [11].

Nonlinear time-history analysis is the most refined tool that can be used for simulating the seismic response of structures such as braced frames. Clearly, in the case of examining the results of shake table tests, time-history analysis with applied base excitation can be used for direct comparison. In practice, however, the choice of seismic records and the large amount of data generated limit its use to specialist applications. In this context, the use of nonlinear static, or pushover, analysis for seismic assessment and design has increased significantly in recent years. It can be employed to assess overall capacity and stability, and to identify the likely plastic mechanisms and associated dissipative regions. The attractiveness of pushover analysis stems mainly from its relative simplicity, in terms of modelling and computational demands as well as interpretation of results, in comparison with nonlinear dynamic analysis [12].

In this paper, observations and findings from shake table tests on full-scale assemblages representing a single storey of a concentrically-braced frame are evaluated in the context of nonlinear pushover and time-history analyses of the test frames. In particular, comparative assessment between the numerical simulations and the experimental results in terms of stiffness, resistance, overstrength and ductility demand experienced by concentrically-braced frames undergoing strong earthquake ground motion is carried out. These tests and analyses form part of a broader research programme investigating the earthquake response behaviour of concentrically-braced frames with steel and composite bracing members of varying slenderness [13]. In this paper, the experimental and analytical responses of three test frames employing steel braces with a range of slenderness are compared.

2. Experimental model and test set-up

The experimental set-up employed in the shake table tests is shown in Fig. 1 and a view of a test frame installed on the shake table prior to testing is shown in Fig. 2. The concentrically-braced single storey test frame has an overall height of 2.89 m, and plan dimensions of 2.70 m×2.47 m, supporting a test mass of approximately 10 000 kg. A pair of brace specimens were employed in each test to simulate the interaction between the tension and compression braces that occurs in real structures subjected to earthquake excitations. The two braces were not connected at mid-length, but were sufficiently separated in plan in order to avoid contact in the event of out-of-plane buckling. This arrangement accounts for the load sharing interaction that occurs between the braces within a typical storey of a concentrically-braced frame. However, it does not represent additional interaction effects that may influence the assessment of buckling lengths in inter-connected brace configurations. Further details of the test frame are provided by Elghazouli et al. [13].

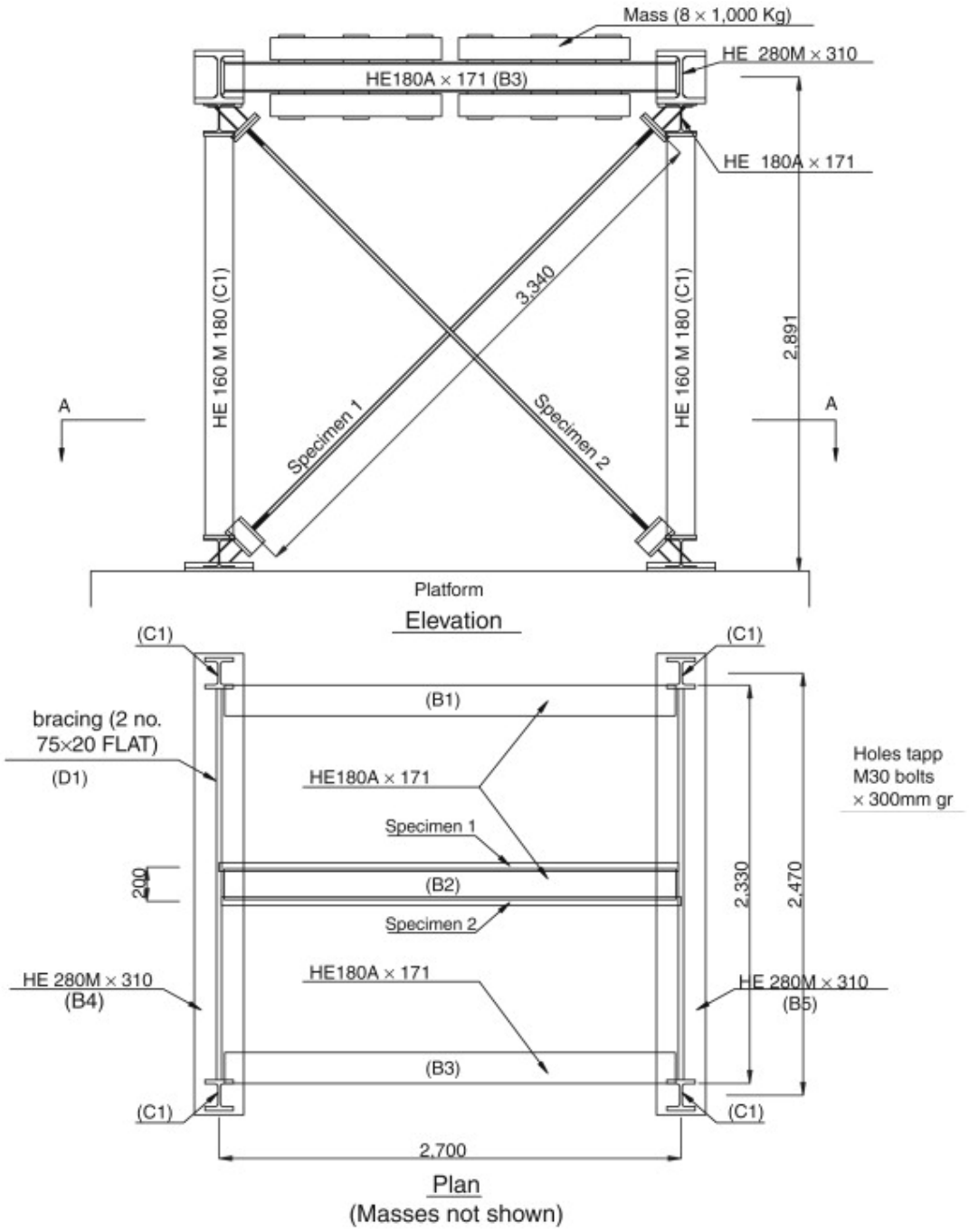

Fig. 1. Shake table test model and experimental set-up.

Fig. 2. View of test frame on shake table prior to testing.

In total, 36 shake table tests were conducted on ten pairs of hollow and filled bracing members [13]. Braces with three different cold-formed square and rectangular hollow cross-section sizes were examined (20×20×2.0, 50×25×2.5 and 40×40×2.5). These sizes were selected to provide a range of section and member slenderness within the capacity of the shake table. In this paper, the response of three frames (one from each brace size) are considered; details of these are provided in Table 1.

Table 1. Test frame properties and loading

Test ID	Brace cross-section (mm)	λ	f_y (N/mm²)	f_u (N/mm²)	f_n (Hz)	Input	Max. table acceleration
ST2	50×25×2.5	2.2	332.9	354.5	4.68	El Centro	$0.81g$
ST4	20×20×2.0	3.0	283.1	345.9	3.99	Cyclic	$1.01g$
ST8	40×40×2.5	1.6	395.9	435.4	6.05	El Centro	$2.01g$

Table options

In each test, both brace members were fabricated from the same length of steel, ensuring symmetrical frame properties. The yield and ultimate strengths of the specimens as determined from tensile tests on specimens cut from these lengths of steel are given in Table 1. The end detail of each brace member employed an 8 mm thick stiffener plate (125 mm long and 100 mm wide), which was placed through slots in the centre of two of the opposing faces of the section. This plate was welded to the hollow section and both the plate and the hollow section were welded to 20 mm thick end plates. At the lower end of the braces, these end plates were joined to load cells using 12 bolts of 16 mm diameter. At the upper end of the braces, the end plates were connected to HE 280M × 310 transverse beams (B4 and B5 in Fig. 1), again using 12 bolts of 16 mm diameter. Based on this design, all braces possessed a clear length of 3050 mm under nominally rigid end conditions. When combined with the measured material strength, this leads to the normalised slenderness ratio shown in Table 1. The normalised slenderness is defined by Eurocode 3 [14] as

equation(1)

$$\lambda = \sqrt{N_{pl}/N_{cr}}$$

in which N_{pl} and N_{cr} are the plastic section capacity and the elastic (Euler) buckling load, respectively.

The transverse beams supported three longitudinal beams (B1–B3 in Fig. 1) whose function was to support eight one-tonne test masses. Including the weight of the beams and other components, the total mass above the top of the columns was 10 114 kg. The column members (C1 in Fig. 1) comprised HE 160M × 180 sections that were fixed to the table platform and the transverse beams using short lengths of HE 180A × 171 steel sections, as shown in Fig. 1. The flexibility of the web of these sections ensured that the columns were effectively pinned at both ends.

Elastic tests employing low-amplitude random input motion indicated average fundamental natural periods of vibration of about 0.26, 0.18 and 0.16 s for the frames with 20×20×2.0, 50×25×2.5 and 40×40×2.5 braces, respectively. The actual fundamental period of vibration of each frame was found to depend on both the slenderness and the initial out-of-straightness of the brace members. The typical critical damping ratio was just over 3%. Large-amplitude inelastic tests examined the post-buckling and post-yield behaviour of the bracing members. For two of the tests considered here (ST2 and ST8), the shake table excitation used was a scaled acceleration history from the North–South component of the Imperial Valley record of the 1940 El Centro earthquake. The original record, with a peak ground acceleration of about$0.34g$ was appropriately scaled for either frame depending on the expected strength of the brace members, as indicated in Table 1. In Test ST4, the shake table motion followed a sinusoidal ramp function with a frequency equal to 80% of the measured fundamental frequency of the test frame (f_n in Table 1) and an amplitude sufficient to ensure inelastic response of the brace members. Detailed discussions of the results and observations from the shake table tests are presented elsewhere 13. and 15..

3. Numerical model and procedures

Earthquake structural analysis was performed using the nonlinear finite element analysis program ADAPTIC [16] which accounts for material and geometric nonlinearities. A two-dimensional model of the test frame, illustrated in Fig. 3, was developed with a view to accurately representing the inelastic tensile and buckling behaviour of the brace members. Each brace member was modelled using 10 cubic inelastic fibre elements whose cross-sections are divided into a number of monitoring areas. A strain-hardening bilinear stress–strain material law was selected for the analysis carried out in this investigation. This relationship is imposed at each time- or load-step while ensuring equilibrium with global member forces. The members capture the alternating tensile yielding/elongation and flexural buckling exhibited by the braces.

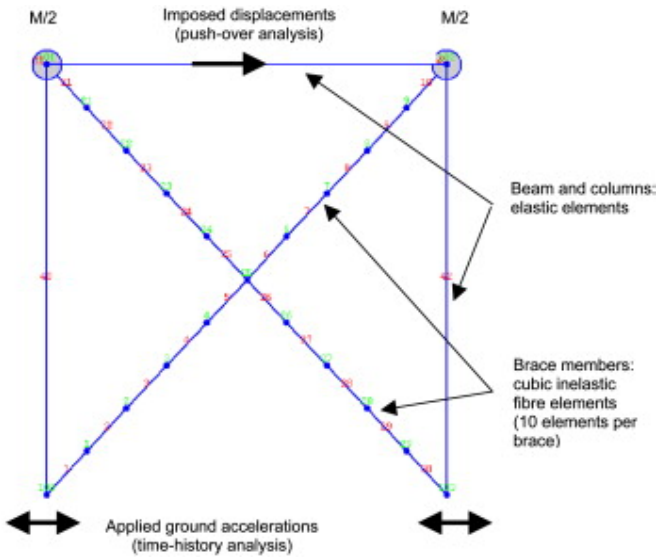

Fig. 3. Analytical model.

The brace members are rigidly connected to the rest of the structural model which comprises two elastic column members both supporting 50% of the 10 000 kg test mass at their upper ends, joined through pinned connections to the shake table platform and a connecting beam member. Different models were created for each test frame, using individual brace dimensions, actual brace yield strengths measured in tensile tests, and viscous damping measured in low-amplitude tests.

This model was employed in two types of earthquake response analysis. In time-history analyses, the ground accelerations imposed during each shake table test (Table 1) were applied to the nodes where the columns and brace members were attached to the shake table platform. The resulting response of the frame was calculated using a time-stepping technique employing the widely-used Newmark numerical integration scheme with a time-step of 0.01s and internal iterations within each time-step. A viscous damping representing 3% of the critical was used throughout the time-history analysis. Due to possible differences between the target and applied input excitations in the tests, the numerical simulations were carried out using the actual acceleration histories measured on the table. In pushover analyses, the base of the frame was held in position while the top nodes were translated horizontally in a series of incremental applied displacements. For each displacement-step, the equilibrium of the internal member forces and overall frame base shear was ensured through a number of iterations.

4. Transient experimental and numerical response of test frames

4.1. Acceleration time history

Fig. 4 compares the experimental and analytical (time-history) acceleration responses of Test ST4. The imposed table acceleration function is also shown. During the first second of the test, both the measured and calculated responses increase in line with the table acceleration. Thereafter, the peak

acceleration response is limited due to yielding of the brace members. The dotted lines on these graphs indicate the expected peak acceleration suggested by the measured tension capacity of the brace members.

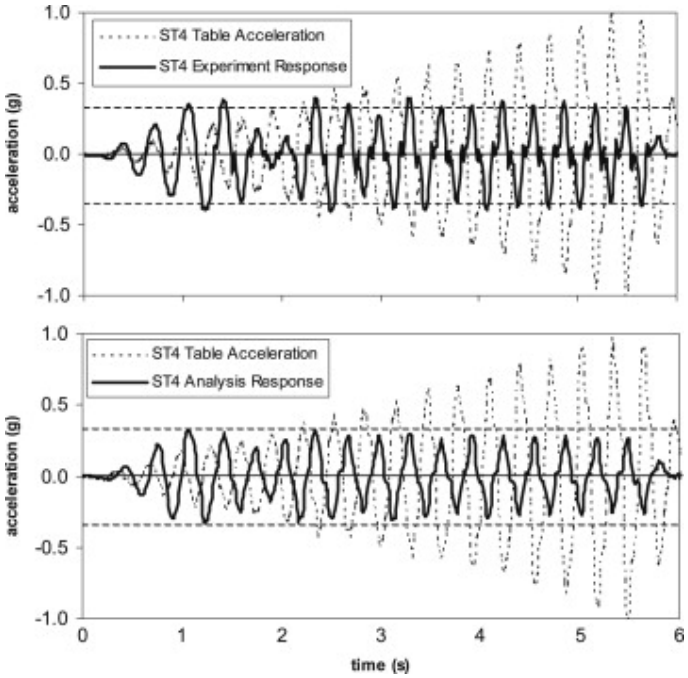

Fig. 4. Experimental and analytical acceleration response of Test ST4.

An important aspect of the response of concentrically-braced frames is displayed just before two seconds of the test have elapsed. The peak acceleration is reduced over two successive cycles because both braces remain in a post-buckled state, without completely straightening. This is attributable to the non-recoverable plastic lengthening of the brace members that occurs following yielding. In later cycles the response is greater, straightening the braces early enough to allow yielding to occur before unloading begins. Fig. 5 illustrates how this behaviour is displayed in the experimental axial force–displacement response of brace members subjected to cyclic axial loading [15]. The brace member referred to in Fig. 5(a) is of size 40×40×2.5 and a slenderness $\bar{\lambda}$ of 1.3, whilst that in Fig. 5(b) is of size 50×25×2.5 and a slenderness $\bar{\lambda}$ of 1.9. It is clear that the tension capacity of the brace is realised only once at each displacement amplitude, with subsequent cycles at the same amplitude displaying lower resistance. This behaviour is displayed by braces of any slenderness 4., 5. and 6., but as shown in Fig. 5, the tangent stiffness of the brace varies continuously in a manner that does depend on slenderness.

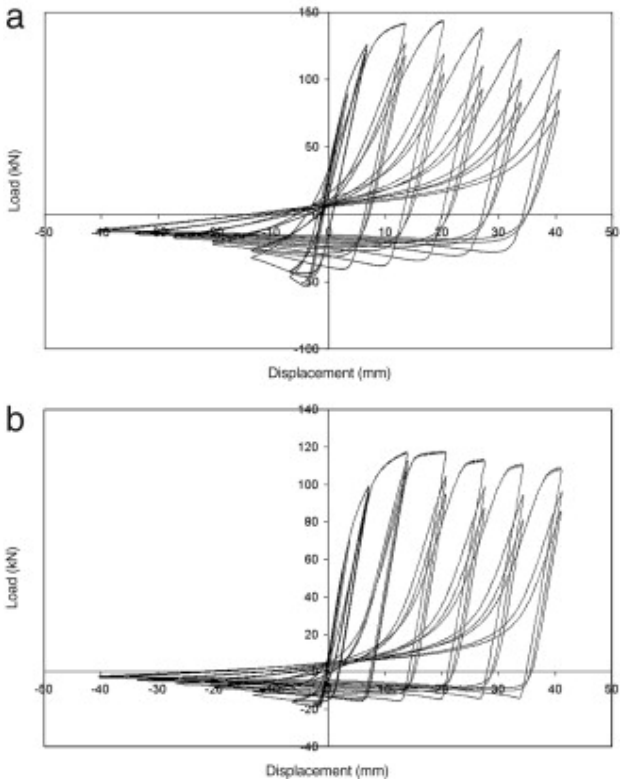

Fig. 5. Experimental cyclic axial load–displacement response of two hollow brace members $L = 3300$ mm: (a) 40×40×2.5 SHS ($\lambda = 1.4$), (b) 50×25×2.5 RHS ($\lambda = 1.9$).

Fig. 4 indicates that the analytical model successfully captures this behaviour in time-history response analysis of the response of the frame to harmonic ground motion. Fig. 6 and Fig. 7 examine the ability of the model to capture the response of two frames, with braces of different slenderness, that are subjected to recorded earthquake accelerations. Fig. 6 compares the experimental and analytical acceleration responses of Test ST2 which examined the response of a frame with slender braces (50×25×2.0RHS, $\lambda = 2.2$) to scaled El Centro ground motion. Very good agreement is observed during the first half of the test, with similar peak accelerations observable in the experimental and analytical plots. However, the accelerations are substantially reduced in the latter half of the experimental response, partly due to smaller ground motions, but mostly due to plastic elongation of the brace members, as observed in Test ST4 above. A similar response reduction is also displayed in the second half of the analytical response plot, but the peak accelerations are greater than those in the experimental case. Some local buckling occurred in the brace members after approximately 14 s of the test had elapsed. This aspect of behaviour is not incorporated in the numerical model, hence this may have also contributed to the difference between the experimental and analytical responses observed towards the end of the test.

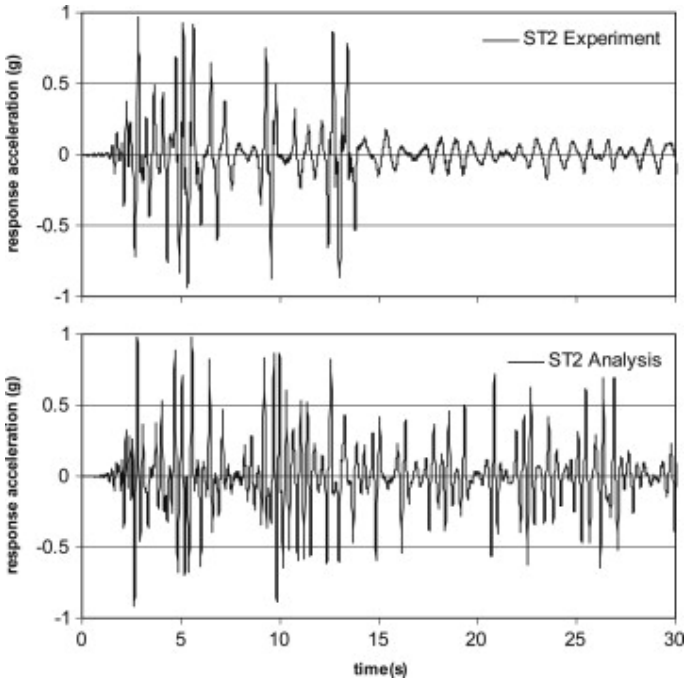

Fig. 6. Experimental and analytical response acceleration of Test ST2.

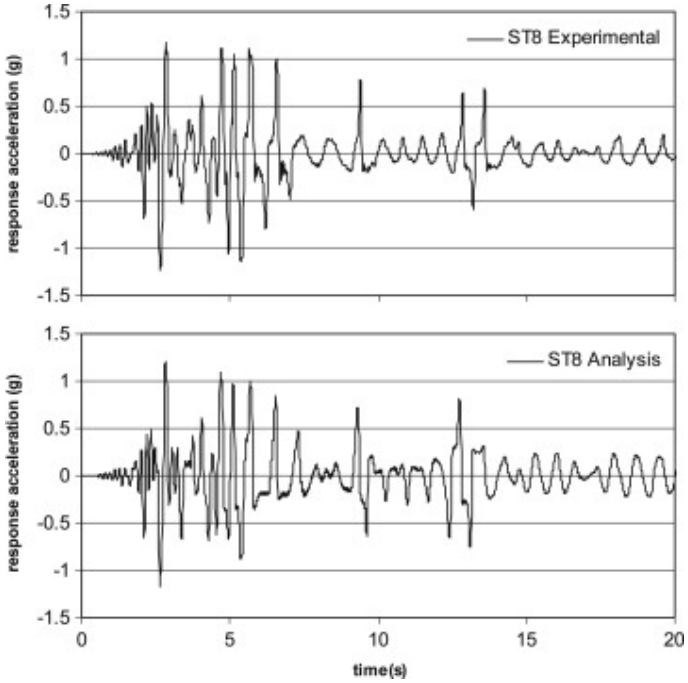

Fig. 7. Experimental and analytical response acceleration of Test ST8.

This behaviour is examined in more detail in Fig. 8 where wavelet coefficients calculated from the transient experimental acceleration response of test ST2 are presented. Wavelet transformation is a process for determining how well a series of wavelet functions represents a transient signal, with the level of similarity between the wavelet functions and the signal being quantified by wavelet

coefficients [17]. The measured response of test ST2 was decomposed into its wavelet components using

equation(2)

$$W_{\psi} f(a,b) = \frac{1}{\sqrt{a}} \int_{-\infty}^{\infty} f(t) \psi^{*}\left(\frac{t-b}{a}\right) dt$$

where the wavelet transform $W_{\psi} f(a,b)$ correlates the signal function $f(t)$ (the frame acceleration response) with the wavelet function $\psi_{a,b}(t)$, with $\psi^{*}(\cdot)$ denoting the complex conjugate of the wavelet function. The Littlewood–Paley or harmonic wavelet proposed by Newland [18], was employed for $\psi(t)$, given by

equation(3)

$$\psi(t) = \frac{1}{\pi} \frac{\sin(2\pi t) - \sin(\pi t)}{t}.$$

The frequency range and duration of the wavelet function are varied by selecting appropriate values of the parameters a and b. The wavelet coefficients calculated for four frequency ranges in the vicinity of the natural frequency of the test frame are shown in Fig. 8. In physical terms, the amplitudes of these plots indicates how the natural frequency of the frame changes throughout its response. It can be seen that during the first 15 s of the test, the response is rich in frequency components above 2 Hz, but these components subsequently disappear. The frequency component in the range 1–2 Hz also reduces considerably after 15 s. In contrast, the wavelet coefficients in the 0.5–1 Hz plot increase as the test progresses, reflecting a reduction in the fundamental frequency of the frame from its initial elastic value of 4.68 Hz (Table 1). This change in frequency is due to the lengthening of both braces during the early strong ground motion phase of the test, and subsequent loss of stiffness as the braces maintain their post-buckled shape and are unable to provide tensile resistance during lateral frame oscillations.

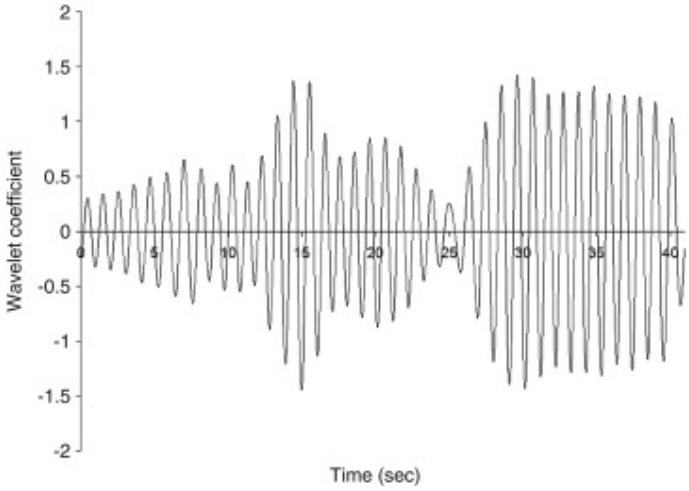

(a) 0.5–1 Hz.

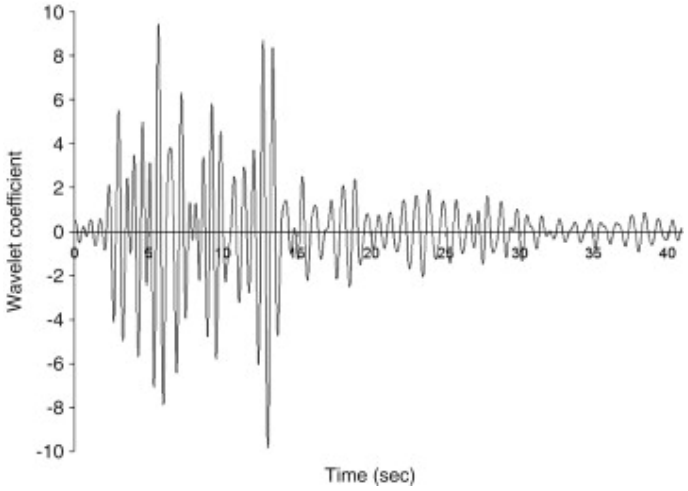

(b) 1–2 Hz.

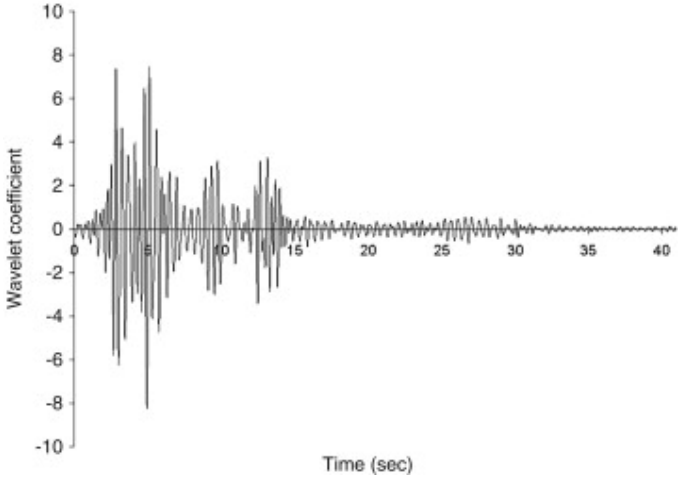

(c) 2–4 Hz.

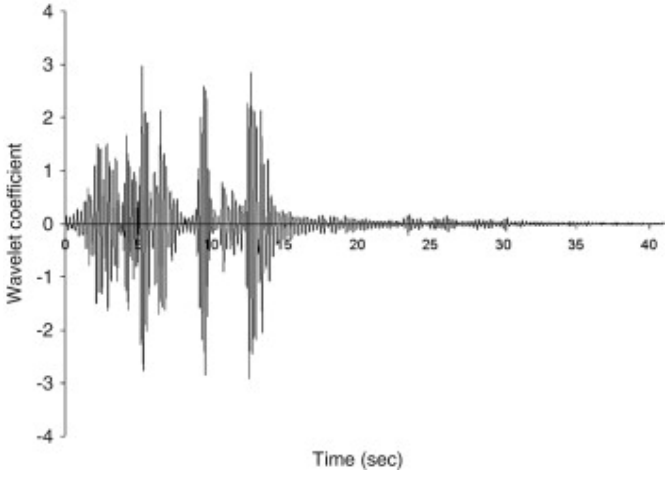

(d) 4–8 Hz.

Figure 8. Wavelet coefficients for the response of test ST2

Very good agreement between the experimental and analytical acceleration responses of frame ST8 is observed in Fig. 7. The times and amplitudes of the acceleration peaks measured in the test are

accurately predicted by the analytical model, as is the low-amplitude response observed between 15 and 20 s.

4.2. Transient brace force response

Fig. 9 and Fig. 10 compare the experimental and analytical axial brace force responses in tests ST4 and ST2, respectively. The responses of both braces in each test frame are presented, and the relationship between brace resistance and frame acceleration can be examined through comparison withFig. 4 and Fig. 6. Horizontal lines indicate the expected tensile capacities and Euler buckling loads determined using measured brace strengths and dimensions. In Fig. 9, the lowest brace forces during test ST2 are observed between 1.5 and 2.0 s of the response, coinciding with the reduced frame accelerations displayed in Fig. 4. It is clear that during these cycles, neither brace is stretched sufficiently to cause tensile yielding. This behaviour is predicted by the analytical model, albeit with some differences in peak force values. Fig. 10 shows that with the more irregular El Centro earthquake loading used in test ST2 the brace forces predicted by the analytical model generally agree with those observed experimentally, but they also display a tendency to overestimate the measured response at some points, for the reasons outlined previously.

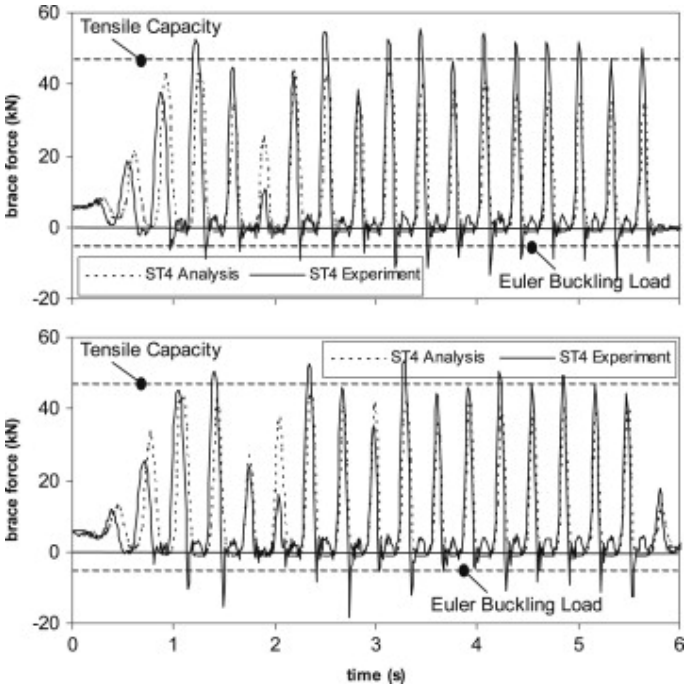

Fig. 9. Experimental and analytical time-histories of brace axial forces during Test ST4.

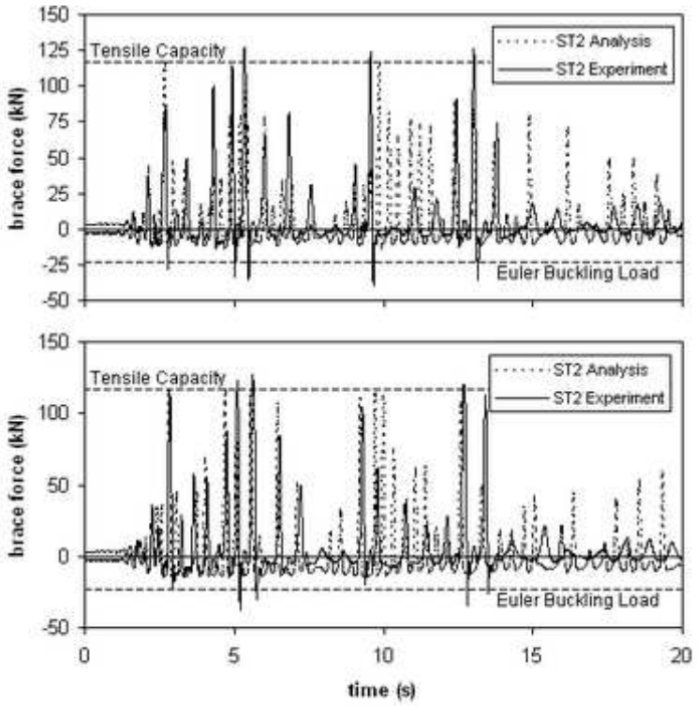

Fig. 10. Experimental and analytical time-histories of brace axial forces during Test ST2.

The actual measured material strength of the brace specimens was utilised in the analytical model of each test frame. These strengths were determined in quasi-static tensile tests on short specimens that included the entire cross-section of the member, thereby capturing the increment to section capacity caused by cold-forming [15]. Nevertheless, although the tension brace forces predicted in the time-history responses generally agree with those measured during the shake table tests, the highest brace forces tend to be underpredicted — by 11% in the cyclic test ST4, and by 9% and 12% in tests ST2 and ST8, respectively. This result is of importance, because as part of capacity design approach, nonlinear time-history analysis can be used to determine design action effects for the nondissipative elements of a braced frame, such as connections and columns. The comparison of observed and predicted responses presented here suggests that analytical results should not be employed directly in this manner without applying an additional overstrength factor. A more detailed examination of the brace member overstrength observed in cyclic and shake table testing is provided elsewhere [19]. Nonlinear time-history analysis does not predict the sharp peaks in compression forces observed in the shake table tests following rapid brace unloading after large tensile elongation, which is an area that seems to require further investigation.

4.3. Displacement time history

The prediction of transient brace forces using time-history analysis does not provide very useful information on the likelihood of structural failure. This is better addressed by examining global and local deformation demands experienced under earthquake loading, and comparing these with the expected deformation or ductility capacities of the dissipative elements of the steel frame — in this case the bracing members. Reliable information on ductility capacity, and the design and dimensioning required to achieve adequate ductility capacity, is nearly always obtained from quasi-static cyclic or shake table testing, rather than through numerical analysis.

Global displacement ductility demands, calculated as the ultimate lateral frame deformation normalised by the estimated lateral displacement at yield, as high as 13 were experienced during the shake table tests [13]. Many of the test frames experienced ductility demands greater than 6 without failure, with brace failure only occurring with ductility demands of the order of 14 or more. Of the test frame responses to recorded earthquake ground motions considered here, ductility demands of 7.7 and 13.8 were experienced in tests ST2 and ST8, respectively, with brace fracture occurring in test ST8. The ultimate failure mode of the hollow bracing members was observable in test ST8, as illustrated in Fig. 11. Following brace buckling, local buckling occurred at mid-length and close to the fixed brace ends, causing high strains to develop in the corner regions of the cross-section, where the steel exhibits a reduced fracture strain due to cold-working. Cracks eventually formed in these regions, and gradually propagated through the cross-section under repeated cyclic loading.

Fig. 11. Fracture damage to brace of Test ST8.

The initiation of local buckling and fracture is influenced by the width-to-thickness ratio of the elements of the cross-section, as well as the applied loading history. There is also a strong dependence on brace slenderness, since for a given level of lateral deformation, higher curvature arises in plastic hinges that form in members with relatively low slenderness [19]. The brace failure in Test ST8 can therefore be attributed to a combination of relatively low member slenderness and high width-to-thickness ratio, coupled with a significant ductility demand.

Earthquake response analyses of the type considered in this paper do not seek to model the detailed failure of individual components of building frames, such as brace members. Instead, the goal is to predict the global displacement response of the whole structure and the deformation demand experienced by individual members. The challenge arises because local and global deformation demands are inter-dependent and strongly influenced by response history. Fig. 12 presents the experimental and analytical time-histories of the displacement responses of frames ST4 and ST8.

Frame displacement is represented as the relative displacement of the top of the test frame and the shake table platform. For the cyclic loading case shown in Fig. 12(a) there is good agreement between the time-history analysis results and the measured displacement response. However for test ST8 (in Fig. 12(b)), which employed the El Centro earthquake record, the amplitude of the experimental response is underestimated by the numerical model, and the observed asymmetric lateral drift of the frame ST8 was not present in the analysis. This is partly attributed to the initiation of local buckling at an early stage in the test, a criterion which is not represented within the beam elements selected in this study.

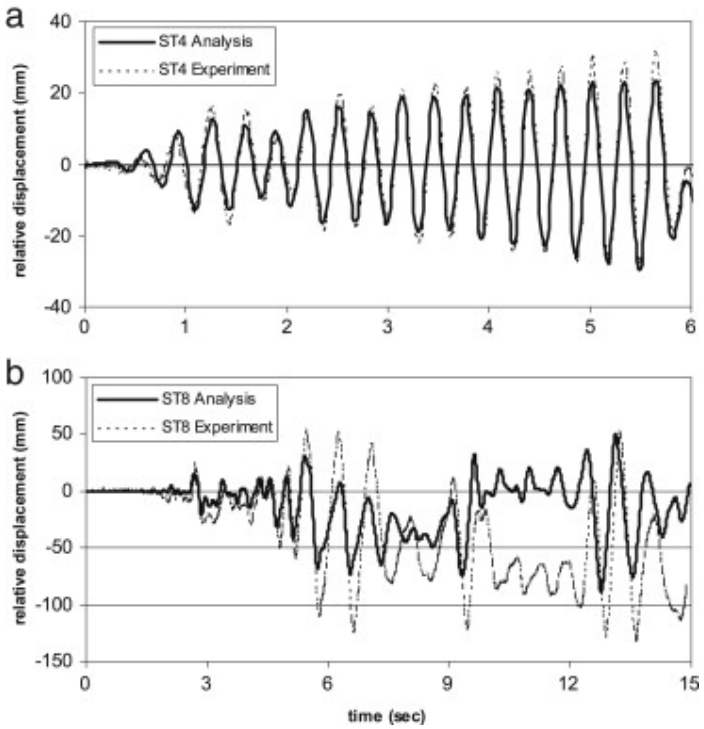

Fig. 12. Experimental and analytical displacement responses of (a) Tests ST4 and (b) Test ST8.

Table 2 compares the maximum relative displacements and ductility demands experienced in the earthquake tests ST2 and ST8 with those identified from the time-history analyses, the results of response spectrum analyses, and design displacement predictions. These results consider the first 20 s of the experimental and numerical response. The spectral analysis displacements, Δ_{sa}, were calculated using the natural frequencies of the test frames measured in elastic tests employing low-amplitude random input motion with the measured peak table acceleration and 5% damping. The ductility demands experienced in the time-history analyses, μ_{th}, were determined by dividing the predicted maximum displacement, Δ_{th}, by the yield displacement identified in pushover analyses (Fig. 13 and Fig. 14). The predicted design ductility demands, μ_{dp}, were based on the equal energy idealisation, which leads to

equation(4)

$$\mu_{dp} = [(V_e / V_y)^{0.5} + 1]/2$$

in which V_e is the elastic storey shear given by
equation(5)
$$V_e = 2.5 M_{test} a_{max}$$

where M_{test} is the test mass, a_{max} is the maximum ground (i.e. table) acceleration and a response acceleration amplification factor of 2.5 has been assumed for a system with 5% damping, while V_y is the design yield storey shear obtained from the measured tensile strengths of the bracing members given in Table 1. The predicted design displacements, Δ_{dp}, were obtained from
equation(6)
$$\Delta_{dp} = (\mu_{dp} \Delta_{ep}) / (2\mu_{dp} - 1)^{0.5}$$

where Δ_{ep} is the predicted elastic displacement given by
equation(7)
$$\Delta_{ep} = V_e / k_f$$

in which k_f is the elastic frame stiffness obtained from the measured natural frequency of the test frame, f_n
equation(8)
$$k_f = 4\pi^2 f_n^2 M_{test}$$

Table 2. Predicted maximum relative displacements and ductility demands

Test	Maximum relative displacement (mm)				Maximum ductility demand		
	Test Δ_{test}	Time history Δ_{th}	Spectral analysis Δ_{sa}	Design prediction Δ_{dp}	Test μ_{test}	Time history μ_{th}	Design prediction μ_{dp}
ST2	61	18	19	33	5.6	2.0	4.1
ST8	131	89	65	92	12.6	9.9	12.8

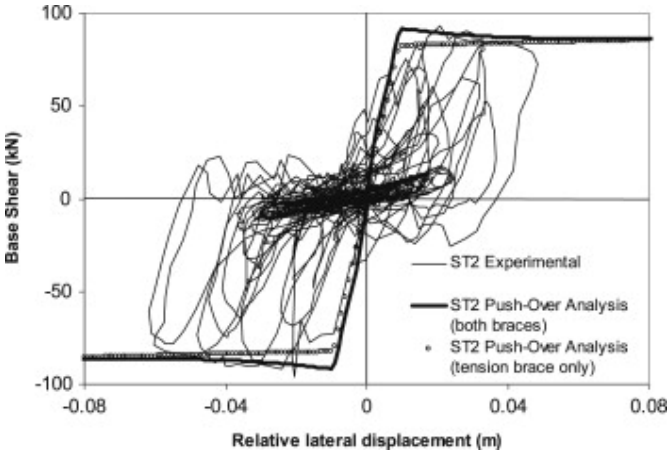

Fig. 13. Lateral displacement–base shear response of Test ST2; comparison of experimental hysteresis response with results of pushover analyses.

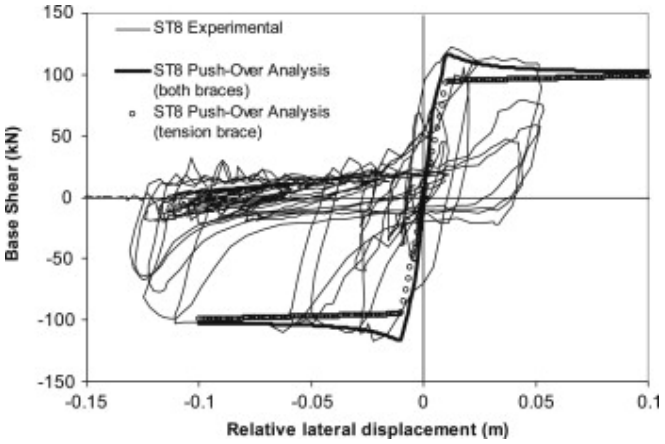

Fig. 14. Lateral displacement–base shear response of Test ST8; comparison of experimental hysteresis response with results of pushover analyses.

For test ST2, there is considerable difference between the maximum relative displacement values shown in Table 2. For this test, the maximum relative displacement determined using time-history analysis agrees well with that obtained using response spectrum analysis, but both of these greatly underestimate the measured experimental value. The design displacement prediction lies closer to the test result. The maximum ductility demand results display a similar trend. For test ST8, all methods underestimate the measured peak response, but by a much smaller margin. In this case, the time-history analysis result and the design prediction are very similar, whereas spectral analysis gives the lowest estimate. The maximum ductility demand experienced in this test agrees well with that displayed in the time-history analysis and, especially, with the design prediction. The good performance of the design prediction approach can be partly attributed to its use of the measured natural frequency of the test frames to determine their initial stiffness.

These results emphasise how small differences between analytical and experimental responses displayed under symmetric loading, such as in Fig. 12(a), can lead to greater divergence under real earthquake conditions, such as in Fig. 12(b). From a design point of view, seismic codes of practice such as Eurocode 8 usually impose an upper bound on the inter-storey drift in a frame at the ultimate limit state. The comparison of experimental and analytical frame displacements suggests that caution is required if the results of time-history analyses are used to verify the drift performance of a frame design.

4.4. Hysteretic frame response and pushover analyses

The maximum shear force developed within a building storey determines the overall lateral capacity of the frame, as well as the force transmitted to other parts of the structure. In multi-storey frames, earthquake resistant design codes normally require an accurate assessment of this force, and its comparison with the resistance of adjacent stories so that a regular distribution of inelasticity is achieved. In the test frames, the storey (or base) shear at any point in the response depends on the combined resistance of both braces, which may be in their elastic, post-buckled or yielded states. The variations of storey shear with frame displacement throughout the three tests considered are

represented as hysteresis plots in Fig. 13,Fig. 14 and Fig. 15. These plots indicate the level of ductility demand experienced in each test, and the large deformations experienced in test ST8 are clear from Fig. 14, as is the asymmetric nature of the response.

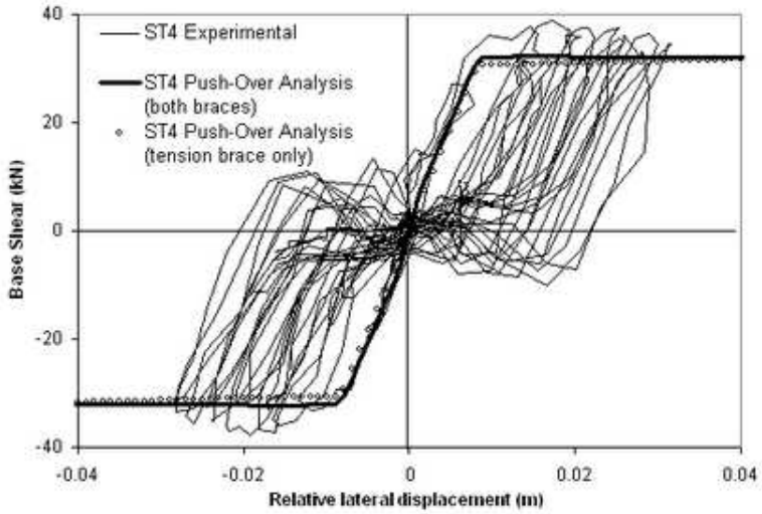

Fig. 15. Lateral displacement–base shear response of Test ST4; comparison of experimental hysteresis response with results of pushover analyses.

Also shown in Fig. 13, Fig. 14 and Fig. 15 are the results of inelastic static or 'pushover' analyses of the test frames. Two cases are shown: one in which both braces are included in the structural model, and another in which the Eurocode 8 design assumption of ignoring the contribution of the compression brace is employed. For tests ST2 (Fig. 13) and ST8 (Fig. 14), the maximum storey shear is well predicted by the nonlinear pushover analysis that considers the resistance of both braces. This is true at all levels of displacement, with the analytical curve providing an accurate envelope of the test forces, even for the large deformation demand experienced in test ST8. In contrast, an analysis based on the resistance of the tension brace alone leads to a consistent underestimate of storey shear, which not surprisingly, is greater for lower slenderness.

Considering all frames tested, experimental and analytical results indicate that for braces with normalised slenderness between 1.5 and 2.4, the ultimate resistance of the frame can be estimated from the maximum tensile strength of the tension brace plus 30% of the compression brace buckling capacity, in line with Eurocode 8 provisions for the design of beams in frames with V-bracings. Only for very slender brace members ($\bar{\lambda} \geq 2.4$, outside the range normally considered for design) should the post-buckling resistance of the compression brace be ignored [15]. In Test ST4, which examined the response of a frame with very slender braces of this kind, the pushover analysis resistance curve does not provide an accurate envelope of the experimental hysteresis plot. A similar underprediction of the resistance of this test frame was observed, as indicated in Fig. 9, for the brace axial forces calculated using time-history analysis.

5. Conclusions

The response of concentrically-braced frames to significant earthquake loading depends strongly on the asymmetric axial resistance of the bracing members. The prediction of this response requires accurate modelling of the cyclic inelastic response of the members, including buckling capacity, post-buckling resistance, tensile yielding and strain-hardening. In this paper, the experimental response of three single-storey braced frames measured in shake table tests is compared with the results of two different types of inelastic response analysis — time-history analysis and pushover analysis. The test frames considered a range of brace slenderness and were subjected to two different forms of table motion.

The comparison of experimental and analytical results shows that the use of inelastic fibre elements with a bilinear material relationship to represent the behaviour of bracing members leads to accurate modelling of earthquake response, but also indicates areas in which extra attention is required. In two of the three tests examined, the acceleration response of the frame calculated using time-history analysis agreed well with that measured during testing. In particular, the analytical model was able to predict the observed short-term reductions in acceleration response caused by permanent elongation and buckling of the brace members. In the other test, good agreement was only observed for the first half of the test, after which the cumulative effect of local buckling and possible modelling idealisations led to a discrepancy between the experimental and analytical results. Similar levels of agreement were observed at the member level by examining the variation in brace axial force throughout the test.

The prediction of structural collapse using earthquake analysis relies upon an accurate assessment of structural displacements, leading to a quantification of the ductility demand experienced by dissipative elements such as bracing members. For harmonic shake table motion, time-history analysis produced a good, if slightly underestimated, prediction of the variation in lateral frame displacement throughout the test. The slight differences were attributed to strain-rate effects; although these can be incorporated in the numerical model, they are normally considered to be insignificant under typical seismic loading. On the other hand, in testing under recorded ground motions scaled to cause significant seismic response, correlative time-history analyses were in general agreement in terms of force levels but asymmetric drift accumulations were found to be very sensitive to slight variations in modelling parameters. Since seismic assessments are often based on inter-storey drift limits, this aspect needs to be carefully considered in interpreting the results of time-history analysis particularly in the case of concentrically-braced frames.

Pushover analysis results were examined by comparing the predicted inelastic lateral-force–displacement response of the test frames with the hysteretic frame displacement — base shear responses displayed during shake table testing. For two of the three frames considered, the pushover analysis result provided an accurate envelope of the observed hysteresis curve, with slightly better agreement being achieved when both the compression and tension brace were included in the structural model. For the other frame, the analytical results slightly underestimated the maximum resistance displayed during testing, but this agreed with the comparison of the experimental response and time-history analysis. The results also illustrate that the design approach adopted in European

provisions whereby the lateral frame resistance is only based on the tension diagonals provides a reasonable representation of the behaviour within practical ranges of brace slenderness. However, in terms of satisfying the objectives of capacity design, it is important that additional checks are considered to account for possible adverse effects caused by the contribution of the braces in compression.

While a body of research exists on the behaviour of bracing member subjected to quasi-static cyclic loading, there is a notable absence of test data on the dynamic response of full-scale braced frames to strong ground motion. The experimental assessment of full-scale braced frames under realistic earthquake loading is limited by experimental constraints in terms of capabilities and cost. Clearly, there is a strong role to be played by nonlinear analysis in providing parametric studies for examining the likely response of different structural configurations to a variety of ground motions. The comparative assessments presented in this paper indicate that analytical tools which incorporate material and geometric nonlinearities can largely capture the main features related to the seismic behaviour of concentrically-braced frames. Particular attention should however be placed in interpreting the inter-storey drift results in time-history analysis by careful consideration of material idealisation and characteristics of the selected seismic excitations.

References

1. S.C. Goel, A. El-Tayem **Cyclic load behavior of angle X-bracing** Journal of Structural Engineering, ASCE, 112 (11) (1986), pp. 2528–2539
2. K. Ikeda, S.A. Mahin **Cyclic response of steel braces** Journal of Structural Engineering, 112 (2) (1986), pp. 342–361
3. A.K. Jain, S.C. Goel, R.D. Hanson **Hysteretic cycles of axially loaded steel members** Journal of the Structural Division, ASCE, 106 (8) (1980), pp. 1777–1795
4. B.F. Maison, E.P. Popov **Cyclic response prediction for braced steel frames** Journal of Structural Engineering, ASCE, 106 (7) (1980), pp. 1401–1416
5. E.P. Popov, V.A. Zayas, S.A. Mahin **Cyclic inelastic buckling of thin tubular columns** Journal of the Structural Division, ASCE, 105 (11) (1979), pp. 2261–2277
6. E.P. Popov, G.R. Black **Steel struts under severe cyclic loadings** Journal of Structural Engineering, ASCE, 107 (9) (1981), pp. 1857–1881
7. X. Tang, S.C. Goel **Brace fracture and analysis of Phase-I structure** Journal of Structural Engineering, ASCE, 15 (8) (1989), pp. 1960–1976
8. R. Tremblay **Inelastic seismic response of steel bracing members** Journal of Constructional Steel Research, 58 (2002), pp. 665–701
9. M. Elchalakani, X.-L. Zhao, R. Grzebieta **Tests on cold-formed circular tubular braces under cyclic axial loading** Journal of Structural Engineering, ASCE, 129 (4) (2003), pp. 507–514
10. CEN **EN 1998-1, Eurocode 8: Design provisions for earthquake resistance of structures, Part 1: General rules, seismic actions and rules for buildings** European Committee for Standardization, Brussels (2004)

11. A.Y. Elghazouli **Seismic design procedures for concentrically braced frames** Proceedings of the Institution of Civil Engineers, Structures and Buildings, 156 (SB4) (2003), pp. 381–394
12. H. Krawinkler, G.D.P.K. Seneviratna **Pros and cons of a pushover analysis of seismic performance evaluation** Engineering Structures, 20 (4–6) (1998), pp. 452–464
13. A.Y. Elghazouli, B.M. Broderick, J. Goggins, H. Mouzakis, P. Carydis, J. Bouwkamp, A. Plumier **Shake table testing of tubular steel bracing members** Proceedings of the Institution of Civil Engineers, Structures and Buildings, 158 (SB4) (2005), pp. 229–241
14. CEN. ENV 1993-1-1. Eurocode 3: Design of steel structures — part 1-1: General rules and rules for buildings. Part 1.3: General rules — supplementary rules for cold-formed thin gauge members and sheeting. 1992
15. Goggins J. Earthquake resistant hollow and filled steel braces. Ph.D. thesis. Trinity College, University of Dublin; 2004
16. Izzuddin BA. Nonlinear dynamic analysis of framed structures. Ph.D. thesis, University of London; 1991
17. I. Daubechies **An introduction to wavelets** Academic Press, San Diego (California, USA) (1992)
18. D.E. Newland **An introduction to random vibrations, spectral and wavelet analysis** Longman, U.K. (1993)
19. J. Goggins, B.M. Broderick, A.Y. Elghazouli, A.S. Lucas **Experimental cyclic response of cold-formed hollow steel bracing members** Engineering Structures, 27 (7) (2005), pp. 977–989